Equivalent Strain and Stress Models for the Effect of Mechanical Loading on the Permeability of Ferromagnetic Materials

Paavo Rasilo[1,2], Ugur Aydin[2], Floran Martin[2], Anouar Belahcen[2], Reijo Kouhia[3], and Laurent Daniel[4]

[1]Faculty of Information Technology and Communication Sciences, Tampere University, FI-33014 Tampere, Finland
[2]Department of Electrical Engineering and Automation, Aalto University, FI-00076 Aalto, Finland
[3]Faculty of Built Environment, Tampere University, FI-33014 Tampere, Finland
[4]Group of Electrical Engineering Paris UMR CNRS 8507, CentraleSupélec, Université Paris-Sud, Université Paris-Saclay, Sorbonne Université, F-91192 Gif-sur-Yvette Cedex, France

An equivalent strain/stress approach is proposed for modeling permeability change in ferromagnetic materials due to mechanical loadings. The model can be used for transforming complex multiaxial mechanical loadings into equivalent uniaxial loadings parallel to the magnetic field, such that the permeability can be predicted only based on uniaxial measurements. Contrary to earlier approaches, the new definition of the equivalent strain/stress also accounts for shear strain/stress with respect to the magnetic field. The results are shown to match well measurements under multiaxial stresses.

Index Terms—**Magnetoelasticity, strain, stress.**

I. Introduction

MAGNETOMECHANICAL interaction causes additional losses and permeability degradation in electrical machine cores [1]. On the other hand, the same effects can be utilized for harvesting electrical energy from mechanical vibration [2], [3]. Complex multiaxial strains and stresses may occur in such applications, but identification measurements are most commonly available only under uniaxial stress parallel to the magnetic field [4], [5]. A simple way to account for the multiaxial loadings in modeling tools is to reduce them to equivalent uniaxial strains [6] or stresses [7], [8] for which permeability measurements are available. Strain-based approaches are convenient with constitutive laws utilized in displacement-based finite-element solvers. On the other hand, stress is usually known during the identification measurements and in simple statically determined structures. Models formulated in terms of both variables are thus needed.

In this paper, we derive an expression for equivalent strain and stress in ferromagnetic materials starting from a thermodynamic constitutive law. An analytical free energy density function is used for expressing the magnetomechanical coupling. The free parameters of the model are fitted against measurements of $B(H)$ curves from M400-50A electrical steel sheets under uniaxial stress. The purpose of the equivalent strain/stress model is then to obtain an analytical expression for reducing an arbitrary strain/stress tensor into an equivalent uniaxial strain/stress oriented parallel to the magnetic field in such way that the energy density remains unchanged. This equivalent strain/stress can then be used for interpolating the permeability only based on the uniaxial measurements. The proposed methods are validated by measurements from a new rotational single-sheet tester with the capability of applying arbitrary in-plane loadings on steel sheet samples. The main novelty of the proposed equivalent strain/stress approach is its ability of accounting for shear stress with respect to the magnetic field contrary to earlier approaches proposed in [6] and [7].

Manuscript received October 11, 2018; revised December 27, 2018; accepted December 28, 2018. Date of publication January 30, 2019; date of current version May 16, 2019. Corresponding author: P. Rasilo (e-mail: paavo.rasilo@tut.fi).

Color versions of one or more of the figures in this paper are available online at http://ieeexplore.ieee.org.

Digital Object Identifier 10.1109/TMAG.2018.2890407

II. Methods

A. Measurements

A new rotational single-sheet tester was used for measuring magnetization curves from M400-50A electrical sheets under uniaxial and multiaxial loadings. The measurement system and the six-leg steel sheet sample are described in detail in [9]. Let us assume a coordinate system so that the sample lies in the xy plane, the x-axis pointing in the rolling direction (RD). In brief, the six servo motor actuators are used for applying force in the plane of the sample along three independent axes. These three forces can be used for controlling the three in-plane strain components ε_{xx}, ε_{yy}, and ε_{xy} of the strain tensor

$$\boldsymbol{\varepsilon} = \begin{bmatrix} \varepsilon_{xx} & \varepsilon_{xy} & 0 \\ \varepsilon_{xy} & \varepsilon_{yy} & 0 \\ 0 & 0 & \varepsilon_{zz} \end{bmatrix}. \tag{1}$$

ε_{xx}, ε_{yy}, and ε_{xy} are measured by a rosette-type strain gage with 10 mm diameter. Neglecting the ΔE effect, the plane stress tensor σ can be calculated from the measured strains by Hooke's law before the sample is magnetized

$$\boldsymbol{\sigma} = \lambda(\mathrm{tr}\ \boldsymbol{\varepsilon})\boldsymbol{I} + 2G\boldsymbol{\varepsilon} \tag{2}$$

where λ and G are the Lamé parameters derived from Young's modulus $E = 183$ GPa and Poisson's ratio $\nu = 0.34$ and $\boldsymbol{I}$ is the second-order identity tensor.

The sample is magnetized by a three-phase coil system using Elgar SW5250A power amplifier, which is controlled

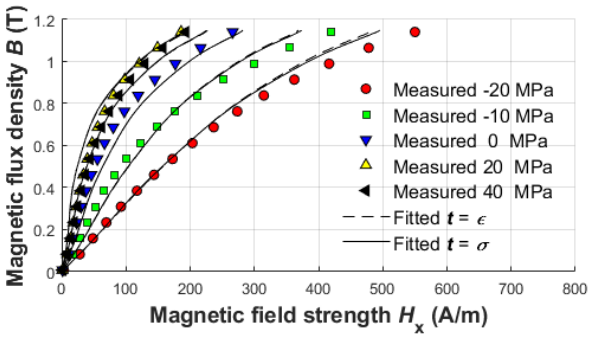

Fig. 1. Fitting of (4)-(6) to magnetization curves measured under uniaxial stresses parallel to the field.

so that a sinusoidally alternating flux density $\boldsymbol{B}$ is obtained in the RD. The x- and y-components of the flux density vector are measured by two 20 mm search coils placed perpendicularly to each other by drilling holes in the middle of the sample. The x- and y-components of the magnetic field strength $\boldsymbol{H}$ from the surface of the sample are measured by two H-coils placed on top of the search coils.

The magnetization curves along RD were measured under uniaxial (subscript uni), equibiaxial (equ) and two shear stress configurations (sh1 and sh2)

$$\boldsymbol{B} = \begin{bmatrix} B \\ 0 \\ 0 \end{bmatrix} \quad \boldsymbol{\sigma}_{\text{uni}} = \begin{bmatrix} \sigma & 0 & 0 \\ 0 & 0 & 0 \\ 0 & 0 & 0 \end{bmatrix} \quad \boldsymbol{\sigma}_{\text{equ}} = \begin{bmatrix} \sigma & 0 & 0 \\ 0 & \sigma & 0 \\ 0 & 0 & 0 \end{bmatrix}$$
$$\boldsymbol{\sigma}_{\text{sh1}} = \begin{bmatrix} \sigma & 0 & 0 \\ 0 & -\sigma & 0 \\ 0 & 0 & 0 \end{bmatrix} \quad \boldsymbol{\sigma}_{\text{sh2}} = \begin{bmatrix} 0 & \sigma & 0 \\ \sigma & 0 & 0 \\ 0 & 0 & 0 \end{bmatrix} \tag{3}$$

where σ varied between -30 and $+30$ MPa. Since only an anhysteretic single-valued material model is considered in this paper, single-valued magnetization curves were extracted from the measured hysteresis loops by averaging the loops in the H-direction. In the case of shear 2, the principal axes of $\boldsymbol{\sigma}$ are not oriented along the RD or TD, and thus, $\boldsymbol{H}$ will have also a non-zero y-component. In the following, only the component H_x along the RD is considered. The measured single-valued $B(H_x)$ curves in the uniaxial case are shown by the markers in Fig. 1. Permeability means the slope of the secant B/H_x. Measurements are available up to 1 T at shear 2 and up to around 1.2 T at the other stress states.

B. Thermodynamic Model

A thermodynamic approach is used for expressing the coupled magnetomechanical constitutive law [10]. A magneto-mechanical free energy density ψ is expressed as a function of the magnetic flux density $\boldsymbol{B}$ and either the strain $\boldsymbol{\varepsilon}$ or stress $\boldsymbol{\sigma}$. The choice of $\boldsymbol{B}$ as the state variable is comfortable if the model is to be used with finite-element formulations based on magnetic vector potential [8]. Denoting the alternative tensor variables by $\boldsymbol{t} \in \{\boldsymbol{\varepsilon}, \boldsymbol{\sigma}\}$, the magnetic field strength is obtained as

$$\boldsymbol{H} = \frac{\partial \psi(\boldsymbol{B}, \boldsymbol{t})}{\partial \boldsymbol{B}}. \tag{4}$$

If an isotropic material is assumed, $\psi(\boldsymbol{B}, \boldsymbol{t})$ can only depend on the following three invariants:

$$I_4 = \frac{\boldsymbol{B}^{\text{T}}\boldsymbol{B}}{B_{\text{ref}}^2}, \quad I_5 = \frac{\boldsymbol{B}^{\text{T}}\boldsymbol{d}\boldsymbol{B}}{B_{\text{ref}}^2}, \quad I_6 = \frac{\boldsymbol{B}^{\text{T}}\boldsymbol{d}^2\boldsymbol{B}}{B_{\text{ref}}^2} \tag{5}$$

where $\boldsymbol{d} = \boldsymbol{t} - (1/3)(\text{tr}\ \boldsymbol{t})\boldsymbol{I}$ is the deviatoric part of the strain/stress $\boldsymbol{t}$ and $B_{\text{ref}} = 1$ T is used only for scaling purposes for simplifying the units.

It is difficult to derive a theoretical expression for the energy density, but the phenomenological model

$$\psi = \sum_{i=1}^{n_\alpha} \alpha_i I_4^i + \beta I_5 + \gamma I_6 \tag{6}$$

has proven to be suitable in many cases. Indeed, Fig. 1 shows the results of least-squares fitting of the model parameters α_i ($n_\alpha = 8$), β, and γ by comparing the measured and modeled $B(H_x)$ curves under five different uniaxial stresses in the RD. The maximum absolute and relative fitting errors are 72.8 A/m and 56% for $\boldsymbol{t} = \boldsymbol{\varepsilon}$ and 62.4 A/m and 55% for $\boldsymbol{t} = \boldsymbol{\sigma}$, but the overall trends are well predicted. The choice of $\boldsymbol{\varepsilon}$ or $\boldsymbol{\sigma}$ as the state variable does not significantly affect the fitting. The obtained parameter values for both cases are given in Table I. Comparison of α_i for both cases shows that the purely magnetic parts of the models remain almost identical. Since uniaxial stress $\boldsymbol{\sigma}_{\text{uni}}$ was used in the measurements, the fitting in the case of $\boldsymbol{t} = \boldsymbol{\varepsilon}$ required iterating correct values for the components of $\boldsymbol{\varepsilon}$ for a given $\boldsymbol{B}$ from

$$\lambda(\text{tr}\ \boldsymbol{\varepsilon})\boldsymbol{I} + 2G\boldsymbol{\varepsilon} + \frac{\partial \psi(\boldsymbol{B}, \boldsymbol{\varepsilon})}{\partial \boldsymbol{\varepsilon}} = \boldsymbol{\sigma}_{\text{uni}} \tag{7}$$

where the first two terms result from (2) and the third term corresponds to the magnetostrictive part of the stress. The obtained strain tensor was then substituted in the place of $\boldsymbol{t}$ in (4). In the case of $\boldsymbol{t} = \boldsymbol{\sigma}$, $\boldsymbol{\sigma}_{\text{uni}}$ was used directly in (4).

TABLE I
MODEL PARAMETER VALUES

Parameter	Case $\boldsymbol{t} = \boldsymbol{\varepsilon}$		Case $\boldsymbol{t} = \boldsymbol{\sigma}$	
α_1	0.0730	J/m^3	0.0729	J/m^3
α_2	-0.287	J/m^3	-0.291	J/m^3
α_3	2.14	J/m^3	2.14	J/m^3
α_4	-7.02	J/m^3	-7.04	J/m^3
α_5	12.5	J/m^3	12.5	J/m^3
α_6	-12.2	J/m^3	-12.2	J/m^3
α_7	6.11	J/m^3	6.13	J/m^3
α_8	-1.24	J/m^3	-1.24	J/m^3
β	-0.874	J/m^3	$-6.24\cdot10^{-12}$	J/m^3/Pa
γ	3746	J/m^3	$1.97\cdot10^{-19}$	J/m^3/Pa^2

C. Equivalent Strain/Stress

We write the flux density vector as $\boldsymbol{B} = B\boldsymbol{b}$, where B is the magnitude and $\boldsymbol{b}$ is a unit vector. The purpose of the equivalent strain/stress model is to transform an arbitrary

strain/stress tensor $\boldsymbol{t}$ into an equivalent uniaxial strain/stress $\boldsymbol{t}_{\mathrm{eq}} = t_{\mathrm{eq}}\, \boldsymbol{b}\boldsymbol{b}^{\mathrm{T}}$ oriented parallel to the flux density. In this paper, the equivalence criteria are defined in terms of the free energy density, so that $\psi(\boldsymbol{B}, \boldsymbol{t}) = \psi(\boldsymbol{B}, \boldsymbol{t}_{\mathrm{eq}})$. Substituting both $\boldsymbol{t}$ and $\boldsymbol{t}_{\mathrm{eq}}$ into (5)–(7) and noting that the first term of (6) only depends on $\boldsymbol{B}$, the equivalence means that

$$\beta \boldsymbol{b}^{\mathrm{T}}\boldsymbol{d}\boldsymbol{b} + \gamma\, \boldsymbol{b}^{\mathrm{T}}\boldsymbol{d}^2\boldsymbol{b} = \frac{2}{3}\beta t_{\mathrm{eq}} + \frac{4}{9}\gamma\, t_{\mathrm{eq}}^2 \tag{8}$$

which can be rewritten as

$$t_{\mathrm{eq}}^2 - 2r t_{\mathrm{eq}} + \frac{9}{4}\boldsymbol{b}^{\mathrm{T}}\left(\frac{4}{3}r\boldsymbol{I} - \boldsymbol{d}\right)\boldsymbol{d}\boldsymbol{b} = 0 \tag{9}$$

where parameter r has been defined as $r = -3\beta/(4\gamma)$. The solution of this quadratic polynomial equation for t_{eq} is

$$t_{\mathrm{eq}} = r \pm \sqrt{\boldsymbol{b}^{\mathrm{T}}\left(r\boldsymbol{I} - \frac{3}{2}\boldsymbol{d}\right)^2 \boldsymbol{b}}. \tag{10}$$

It is noteworthy that $\beta < 0 < \gamma$ which means that $\psi(\boldsymbol{B}, \boldsymbol{t}_{\mathrm{eq}})$ and reluctivity are upward-opening quadratic functions of t_{eq}, which have minimums at $t_{\mathrm{eq}} = r > 0$. Physically, parameter r means the equivalent tensile strain/stress at which the permeability is at maximum. In our measurements, this happens between 20 and 30 MPa, and the parameters in Table I give $r \approx 24$ MPa. The value of r can be conveniently obtained directly from the uniaxial measurements without having to fit parameters α_i, β, or γ, which makes the equivalent strain/stress model (10) easily applicable.

It still has to be determined whether the plus or minus sign has to be chosen in (10). Let us first consider a case with no shear strain/stress with respect to $\boldsymbol{b}$, meaning that $(\boldsymbol{b}^{\mathrm{T}}\boldsymbol{d}^2\boldsymbol{b}) = (\boldsymbol{b}^{\mathrm{T}}\boldsymbol{d}\boldsymbol{b})^2$. This is the case with all other states in (3), except for $\boldsymbol{\sigma}_{\mathrm{sh2}}$. With this condition, (10) becomes

$$\begin{aligned} t_{\mathrm{eq}} &= r \pm \sqrt{r^2 - 3r\boldsymbol{b}^{\mathrm{T}}\boldsymbol{d}\boldsymbol{b} + \frac{9}{4}\boldsymbol{b}^{\mathrm{T}}\boldsymbol{d}^2\boldsymbol{b}} \\ &= r \pm \sqrt{\left(r - \frac{3}{2}\boldsymbol{b}^{\mathrm{T}}\boldsymbol{d}\boldsymbol{b}\right)^2} \\ &= r \pm \left|r - \frac{3}{2}\boldsymbol{b}^{\mathrm{T}}\boldsymbol{d}\boldsymbol{b}\right|. \end{aligned} \tag{11}$$

The last row can be written in two parts as

$$t_{\mathrm{eq}} = \begin{cases} r \pm \left(r - \dfrac{3}{2}\boldsymbol{b}^{\mathrm{T}}\boldsymbol{d}\boldsymbol{b}\right), & \text{if } \boldsymbol{b}^{\mathrm{T}}\boldsymbol{d}\boldsymbol{b} \le \dfrac{2r}{3} \\ r \pm -\left(r - \dfrac{3}{2}\boldsymbol{b}^{\mathrm{T}}\boldsymbol{d}\boldsymbol{b}\right), & \text{otherwise.} \end{cases} \tag{12}$$

It is not physically reasonable that the equivalent strain/stress contains constant terms independent of $\boldsymbol{t}$, and thus, the constant term r should vanish from (12), meaning that the minus sign should be chosen in the upper equation and the plus sign in the lower one, yielding

$$t_{\mathrm{eq}} = \frac{3}{2}\boldsymbol{b}^{\mathrm{T}}\boldsymbol{d}\boldsymbol{b} \tag{13}$$

in the case of no shear stress with respect to the field. This result corresponds exactly to the equivalent stress derived in [7], where the effect of shear stress on the equivalent stress was not considered.

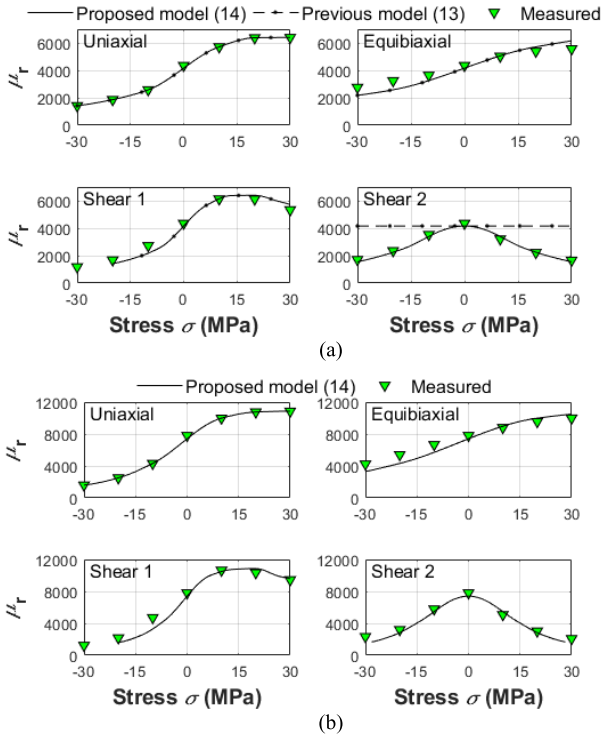

Fig. 2. Comparison of the measured relative permeabilities under multiaxial stresses to those interpolated from uniaxial measurements using the proposed equivalent stress model (14) at (a) $B = 1$ T and (b) $B = 0.5$ T. In (a), the results with the previous model (13) are also shown.

The above-mentioned rule for choosing the sign in (10) will result in a discontinuity in t_{eq} around $\boldsymbol{b}^{\mathrm{T}}\boldsymbol{d}\boldsymbol{b} = 2r/3$ when shear is present such that $(\boldsymbol{b}^{\mathrm{T}}\boldsymbol{d}^2\boldsymbol{b}) \neq (\boldsymbol{b}^{\mathrm{T}}\boldsymbol{d}\boldsymbol{b})^2$. However, since the minimum of $\psi(\boldsymbol{B}, \boldsymbol{t}_{\mathrm{eq}})$ occurs at $t_{\mathrm{eq}} = r$, the energy and permeability are symmetric with respect to $t_{\mathrm{eq}} = r$, and thus, the selection of the sign does not cause discontinuities in the permeability obtained from the model. We thus propose using the above-mentioned rule for choosing the sign and calculating the equivalent strain/stress as

$$t_{\mathrm{eq}} = \begin{cases} r - \sqrt{\boldsymbol{b}^{\mathrm{T}}\left(r\boldsymbol{I} - \dfrac{3}{2}\boldsymbol{d}\right)^2 \boldsymbol{b}}, & \text{if } \boldsymbol{b}^{\mathrm{T}}\boldsymbol{d}\boldsymbol{b} \le \dfrac{2r}{3} \\ r + \sqrt{\boldsymbol{b}^{\mathrm{T}}\left(r\boldsymbol{I} - \dfrac{3}{2}\boldsymbol{d}\right)^2 \boldsymbol{b}}, & \text{otherwise.} \end{cases} \tag{14}$$

III. Application and Results

The proposed equivalent strain/stress approach is tested with the three multiaxial stress configurations $\boldsymbol{\sigma}_{\mathrm{equ}}$, $\boldsymbol{\sigma}_{\mathrm{sh1}}$, and $\boldsymbol{\sigma}_{\mathrm{sh2}}$ shown in (3), when σ varies between -30 and $+30$ MPa. The idea is to obtain the relative permeability $\mu_{\mathrm{r}} = B/(\mu_0 H_{\mathrm{x}})$ under the three stress configurations simply by interpolating from the $\mu_{\mathrm{r}}(\sigma)$ relationship measured under $\boldsymbol{\sigma}_{\mathrm{uni}}$ (markers in the top-left part of Fig. 2(a).

The equivalent stress case $\boldsymbol{t} = \boldsymbol{\sigma}$ is tested first. The maximum permeability point is set at $r = 25$ MPa based on the uniaxial measurements. The three multiaxial stress states are then transformed into equivalent stresses σ_{eq} using (14), and the permeabilities measured in the uniaxial configuration

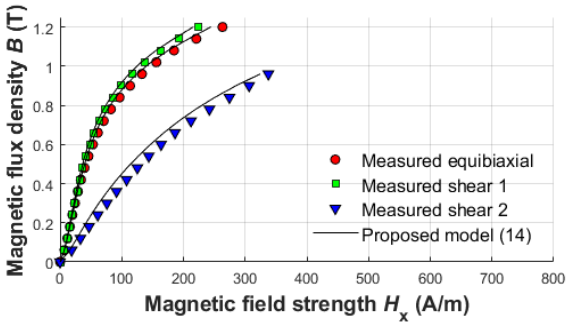

(a)

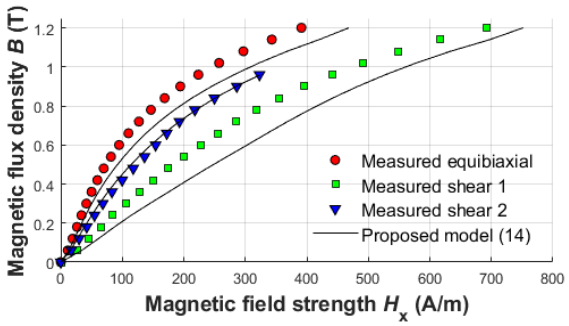

(b)

Fig. 3. Comparison of the $B(H_x)$ curves obtained from the equivalent stress model (14) to those measured with the single-sheet tester under multiaxial loadings (3) when (a) $\sigma = 20$ MPa and (b) $\sigma = -20$ MPa.

are interpolated to these σ_{eq} values. Fig. 2(a) shows that the permeabilities obtained in such way correspond well to the measured permeabilities at $B = 1$ T also in the case of shear 2, which is not accounted for by earlier equivalent stress models. The maximum difference between the model and measurement is 21% at -30 MPa in the equibiaxial case. It is emphasized that no parameter fitting was needed to obtain the results, since the measured value of r was used directly. In the case of shear 1, σ only extends down to -20 MPa, corresponding to an equivalent stress of -30 MPa, which is the maximum compressive stress used in the uniaxial measurements.

The equivalent strain model $\boldsymbol{t} = \boldsymbol{\varepsilon}$ requires first transforming the stress configurations of (3) into equivalent strains by inverting Hooke's law (2) and then applying (14). This needs to be done also for the uniaxial case, since the strain tensor is not uniaxial under uniaxial stress due to the Poisson effect. Parameter r is set to $r = 2(1+\nu)/(3E) \cdot 25$ MPa ≈ 122 μm/m in order to match the value used in the equivalent stress case. The permeabilities measured under $\boldsymbol{\sigma}_{uni}$ are then interpolated to the equivalent strains obtained under $\boldsymbol{\sigma}_{equ}$, $\boldsymbol{\sigma}_{sh1}$, and $\boldsymbol{\sigma}_{sh2}$. The permeabilities at $B = 0.5$ T are shown in Fig. 2(b) and seem to match well with the measured values, the maximum difference being 30% at -10 MPa in the case of shear 1. The results for the equivalent strain and stress models are very similar at both flux density levels and thus not separately shown.

In Fig. 3, the magnetization curves $B(H_x)$ predicted by the equivalent stress model are compared to those measured at the multiaxial stress states (3) when $\sigma = \pm 20$ MPa. In the case of tension, the agreement is good. In the case of compression, notable differences occur in the equibiaxial and shear 1 cases, but the overall trends are well predicted.

IV. Discussion and Conclusion

A new equivalent strain/stress definition was proposed. The model can be used for transforming complex multiaxial mechanical loadings to equivalent uniaxial loadings parallel to the magnetic field such that the permeability can be predicted only based on uniaxial measurements. Contrary to earlier approaches, the new definition also accounts for shear strain/stress with respect to the magnetic field.

Due to the quadratic form of ψ with respect to the strain/stress, the proposed model is mainly suitable for materials in which the permeability increases from the zero-stress value under small tensile stress but decreases in compression and high tension. Such behavior is typically observed in electrical steels. In reality, the permeability does not exactly correspond to a quadratic function, and thus, the discontinuity in t_{eq} caused by the change of sign in (14) may cause a discontinuity in the estimated permeability when both shear normal and shear stresses with respect to the magnetic field are present. However, under the studied multiaxial loadings, the permeabilities were sufficiently predicted.

Although even non-oriented electrical steels show both magnetic and mechanical anisotropy, the assumption of isotropy in the thermodynamic derivations of this paper led to satisfactory results. Accounting for anisotropy in the equivalent strain/stress derivations is a possible topic for future research.

Acknowledgment

The research leading to these results has received funding from the European Research Council under the European Union's Seventh Framework Programme (FP7/2007-2013)/ERC grant agreement no 339380 and from the Academy of Finland.

References

[1] K. Yamazaki and H. Takeuchi, "Impact of mechanical stress on characteristics of interior permanent magnet synchronous motors," *IEEE Trans. Ind. Appl.*, vol. 53, no. 2, pp. 963–970, Mar./Apr. 2017.

[2] S. Cao *et al.*, "Dynamic characteristics of Galfenol cantilever energy harvester," *IEEE Trans. Magn.*, vol. 51, no. 3, Mar. 2015, Art. no. 8201304.

[3] M. Zucca, A. Hadadian, and O. Bottauscio, "Quantities affecting the behavior of vibrational magnetostrictive transducers," *IEEE Trans. Magn.*, vol. 51, no. 1, Jan. 2015, Art. no. 8000104.

[4] A. A. Abdallh and L. Dupré, "The influence of magnetic material degradation on the optimal design parameters of electromagnetic devices," *IEEE Trans. Magn.*, vol. 50, no. 4, Apr. 2004, Art. no. 8000504.

[5] J. Karthaus, S. Steentjes, N. Leuning, and K. Hameyer, "Effect of mechanical stress on different iron loss components up to high frequencies and magnetic flux densities," *COMPEL, Int. J. Comput. Math. Elect. Electron. Eng.*, vol. 36, no. 3, pp. 580–592, 2017.

[6] L. Daniel, "An equivalent strain approach for magneto-elastic couplings," *IEEE Trans. Magn.*, vol. 53, no. 6, Jun. 2017, Art. no. 2001204.

[7] L. Daniel and O. Hubert, "Equivalent stress criteria for the effect of stress on magnetic behavior," *IEEE Trans. Magn.*, vol. 46, no. 8, pp. 3089–3092, Aug. 2010.

[8] K. Yamazaki and Y. Kato, "Iron loss analysis of interior permanent magnet synchronous motors by considering mechanical stress and deformation of stators and rotors," *IEEE Trans. Magn.*, vol. 50, no. 2, pp. 909–912, Feb. 2014.

[9] U. Aydin *et al.*, "Rotational single sheet tester for multiaxial magneto-mechanical effects in steel sheets," *IEEE Trans. Magn.*, to be published.

[10] U. Aydin *et al.*, "Magneto-mechanical modeling of electrical steel sheets," *J. Magn. Magn. Mater.*, vol. 439, pp. 82–90, Oct. 2017.